

# Proton Exchange and Transesterification Reactions of Acetate Enolates with Alcohols in the Gas Phase

Xin Chen and John I. Brauman\*

Department of Chemistry, Stanford University, Stanford, California 94305-5080

Received: May 24, 2005; In Final Form: July 21, 2005

Transesterification reactions and proton exchange reactions between acetate enolates and alcohols were studied both separately and together. Kinetic analysis shows that transesterification and proton exchange happen in a single collision event. The transesterification reaction is best viewed as an endothermic proton transfer, followed by an exchange of alkoxide and an exothermic proton transfer. Reaction barriers were modeled by Rice–Ramsperger–Kassel–Marcus theory and compared to quantum calculations. CBS-QB3 achieves good agreement whereas B3LYP and MP2 give slightly higher barriers. Quantum calculations also predict that the transition state for these transesterification reactions is the same as that for direct transesterification reactions between alkoxides and esters.

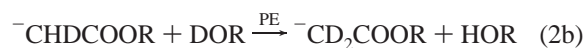
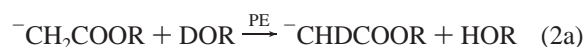
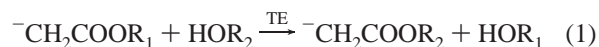
## Introduction

Substituent exchange at carbonyl carbon is of great importance in organic chemistry.<sup>1,2</sup> In solution, these carbonyl addition–elimination reactions proceed through a covalently bound tetrahedral intermediate.<sup>3,4</sup> In the gas phase, interestingly, the reaction potential surface can be either a double well or single well, in which the tetrahedral adduct can be a transition state or simply a complex well.<sup>5–7</sup> If the nucleophiles have high electron affinities, e.g., chloride and bromide, double well potential surfaces with tetrahedral transition states are expected. If the nucleophiles are alkoxides or hydroxides, these transesterification or hydrolysis reactions typically have a single-well potential surface and the tetrahedral adduct is at the bottom of the well with a binding energy of 15–25 kcal/mol.<sup>8</sup>

Transesterification reactions have been studied extensively.<sup>9</sup> Most experiments support the bimolecular base-catalyzed acyl-oxygen cleavage ( $B_{AC2}$ ) mechanism, similar to that in solution.<sup>1,2</sup> Although both experimental and theoretical studies suggest that the tetrahedral adduct in a gas phase transesterification reaction is a minimum, not a maximum, it is not clear if the potential surface has any barrier to reach this minimum. *Ab initio* calculations showed that a very small barrier ( $\sim 1$  kcal/mol) has to be overcome in a similar system, alkaline hydrolysis of carboxylic esters.<sup>10,11</sup> A similar potential surface is expected for transesterification reactions, but the result has not been demonstrated experimentally. Direct transesterification or hydrolysis reactions of esters, usually without acidic  $\alpha$ -hydrogens, have very high efficiencies and are not informative.<sup>5</sup> The reactants have too much energy to be affected by a small barrier more than 10 kcal/mol lower than the reactants.

Transesterification reactions of esters with acidic  $\alpha$ -hydrogens, for example acetate esters, are rarely studied. Acid–base reactions become dominant in this case, as the  $\alpha$ -hydrogen in acetate esters is 4–10 kcal/mol more acidic than alcohols. Klass et al. detected transesterified enolate anions between methoxide and acetate esters.<sup>12</sup> But Vanderwel and Nibbering<sup>7</sup> observed the opposite: only proton transfer but no transesterification occurs when methoxide reacts with methyl acetate. This was

further confirmed and extended to other acetate esters.<sup>9,13</sup> Ultimately, Gross showed that transesterification reactions occur between acetate enolates and alcohols, where  $R_1$  and  $R_2$  are alkyl groups.<sup>9</sup> The transesterification reactions are reversible if both  $HOR_1$  and  $HOR_2$  are present. The equilibrium between enolate anions can be established and basicities of enolate anions can be derived from acidities of alcohols and equilibrium constants. Deuterium labeling experiments showed that proton exchange reactions (PE) occur simultaneously with transesterification reactions (TE).

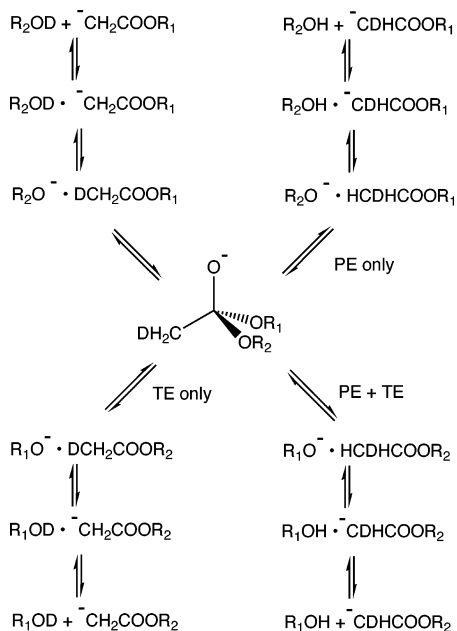


Why is the TE reaction not observed for acetate esters and other esters with acidic hydrogens? Is this prohibited by the small barrier before reaching tetrahedral intermediate? Can this barrier be observed experimentally? What is the relationship between PE and TE of acetate enolates and alcohols?

In this study, we examine the reactions between acetate enolates and alcohols, with both  $\alpha$ -hydrogen and alkyl groups isotopically labeled, so that the products of PE and TE can be simultaneously distinguished and measured by mass spectrometry. Kinetic analysis shows that a TE is always coupled with a PE, whereas a PE can proceed without a TE. Density functional theory (DFT) was applied to study the potential surface of a representative system: methyl acetate plus methoxide. For both PE and TE, the barriers calculated with DFT have to be lowered by  $\sim 2$  kcal/mol to achieve good agreement between Rice–Ramsperger–Kassel–Marcus (RRKM) theory and the experimental rates. CBS-QB3 gives better agreement with experiments. Nevertheless, both theory and experiment suggest that TE rates are determined by the barrier before the tetrahedral intermediate is formed. For methoxide/acetate esters, the RRKM analysis also predicts that the ratio between direct

\* Corresponding author. E-mail: brauman@stanford.edu.

## SCHEME 1: Reaction Mechanism



transesterifications and the acid–base reactions is simply too small to observe any transesterification products.

## Experimental Section

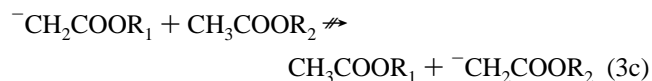
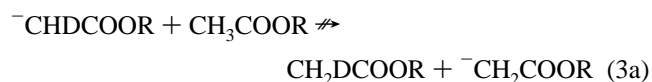
**Instrumentation and Materials.** An IonSpec OMEGA Fourier transform ion cyclotron resonance mass spectrometer (FT-ICR) with impulse excitation was used to measure the reaction rates.<sup>14</sup> Experiments were performed at a 0.6 T magnetic field with a background pressure of  $(1-3) \times 10^{-9}$  Torr. The pressures of the alcohols were measured with a Varian ionization gauge calibrated against a MKS Baratron capacitance manometer. The errors in absolute pressure measurements were estimated to be 30%. The temperature in the ICR cell was estimated to be 350 K.<sup>14</sup>

Nitrogen trifluoride ( $\text{NF}_3$ ) was purchased from Ozark-Mahoning. All alcohols and acetates except methyl acetate- $d_3$  were purchased from Aldrich and used without further purification. Methyl acetate- $d_3$  was synthesized from methanol and acetyl- $d_3$  chloride and purified by preparative GC. Proton NMR (500 MHz) did not detect any impurities. All reagents were introduced into the vacuum chamber through variable leak valves after multiple freeze–pump–thaw cycles. Positive and negative ion spectra showed expected patterns.

**Experiments.** We chose five alcohol–enolate pairs: system 1, methanol- $d_3$  + methyl acetate- $d_3$ ; system 2, methanol- $d_4$  + methyl acetate; system 3, ethanol- $d_6$  + ethyl acetate; system 4, ethanol + ethyl- $d_3$  acetate- $d_5$ ; system 5, butanol- $d_{10}$  + butyl acetate. In these representative systems, we labeled both  $\alpha$ -hydrogen and alkyl groups with deuterium. All enolate ions can exchange one alkyl group (TE) and two hydrogens (PE) with the neutral alcohols, so a total of six ions can be detected, simply by their different masses. In Scheme 1 (system 3 is used as an example), the six ions are designated ion 1 to ion 6, and concentrations of them are noted as C1 to C6, respectively. All reactions are treated as pseudo first order. Without any molar changes in any of these reactions, the total intensity of the six ions can be normalized to unity. Even though these reactions are thermoneutral and reversible, the back reactions do not happen because the concentration of corresponding alcohols is very low. We also tried a few other alcohol–enolate pairs (entries

3, 4, and 10 in Table 1), in which either the  $\alpha$ -hydrogen or alkyl groups were isotopically labeled. Here only PE or TE rates can be measured, and they serve as ideal comparisons to those representative systems.

Electron impact on  $\text{NF}_3$  generates the primary ion  $\text{F}^-$ .  $\text{F}^-$  reacts with acetates to give enolate ions. Other product ions ( $^-\text{CH}_2\text{CFO} < 30\%$  and  $\text{CH}_3\text{COO}^- < 15\%$ ) were ejected at the beginning of the duty cycle. Several studies have shown that the direct proton transfer was the less important channel.<sup>13,15–17</sup> The difference in our work may arise from the kinetic energy of the primary ion,  $\text{F}^-$ . Nearly thermoneutral proton abstraction reactions by  $\text{F}^-$  were shown to have a positive kinetic energy dependence whereas other reaction channels with a tight transition state, such as  $\text{S}_{\text{N}}2$  or E2 reactions, have a negative kinetic energy dependence.<sup>18,19</sup> The opposite kinetic energy dependence results in the different product ratios. In our instrument, the  $\text{F}^-$  directly generated from electron impact dissociation is kinetically hot. When inert buffer gases were added, much of the extra kinetic energy was removed, and the yield of the enolate ions dropped significantly. With the highest buffer pressure we used, direct proton abstraction became the less important channel, though the yield was still about 10%, higher than in previous work. It is possible that H-exchanged ester enolates react back with neutral acetates to exchange H. Fortunately, however, the enolate anions undergo slow proton transfer reactions with ketones or esters.<sup>20</sup> Control experiments were performed. For example, ethyl acetate enolate and ethyl- $d_3$  acetate- $d_5$  ( $1 \times 10^{-6}$  Torr) give neither proton transfer nor transesterification products. The upper limit of these reactions can be estimated to be  $5 \times 10^{-13} \text{ cm}^3 \text{ molecule}^{-1} \text{ s}^{-1}$ .



We used deuterium to discriminate between alkyl groups, though this is not absolutely necessary. However, as shown in Gross's and our data, acetate esters with larger alkyl groups have slightly higher acidities and significantly enhanced rates of TE as well as PE. The alkyl groups differing only in isotopes should have essentially identical rates.

The TE reaction rate constant for methyl acetate enolate + methanol is very slow ( $< 1 \times 10^{-11} \text{ cm}^3 \text{ molecule}^{-1} \text{ s}^{-1}$ ). The reaction times required up to 8000 ms. All others required up to 4000 ms. Ion loss is a significant problem given the elapsed time. The ion balance<sup>21</sup> is  $\sim 85\%$  ( $\sim 75\%$  for systems 1 and 2). Because all six ions have exactly the same chemical structure and very similar masses, we assume that ion loss is proportional to the ion intensity and normalization of intensities will correct the error. This is another advantage of isotope labeling.

Enolate anions are the only products. No complex was generated at the pressure we used. No free alkoxide was detected either. Alcohols are usually 4–10 kcal/mol less acidic than acetates.<sup>22</sup> The proton transfer reactions from alcohols to acetates are too endothermic to occur significantly.

Finally, methoxide and isobutoxide ions, generated by electron impact on methyl peroxide and isobutyl peroxide respectively, were allowed to react with all acetates. The only

**TABLE 1: Experimental Rate Constants, Collision Rate Constants and Efficiencies Obtained at 350 K<sup>a</sup>**

|                 | enolate anion | alcohol   | $k_{PE}^b$                       | $k_{TE}^b$ | $k_{collision}^b$ | Eff <sub>PE</sub> | Eff <sub>TE</sub> | $k_{PE}/k_{TE}$ |      |
|-----------------|---------------|---|----------------------------------|------------|-------------------|-------------------|-------------------|-----------------|------|
| 1               | 1 + 1         | <sup>-</sup> CD <sub>2</sub> COOCH <sub>3</sub>               | CD <sub>3</sub> OH               | 6.2        | .76               | 177               | 0.035             | 0.0043          | 8.0  |
| 2               | 1 + 1         | <sup>-</sup> CH <sub>2</sub> COOCH <sub>3</sub>               | CD <sub>3</sub> OD               | 7.2        | .82               | 178               | 0.041             | 0.0046          | 8.8  |
| 3               | 1 + 1         | <sup>-</sup> CD <sub>2</sub> COOCH <sub>3</sub>               | CH <sub>3</sub> OH               | 5.9        |                   | 183               | 0.032             |                 |      |
| 4               | 1 + 1         | <sup>-</sup> CH <sub>2</sub> COOCH <sub>3</sub>               | CD <sub>3</sub> OH               |            | .88               | 179               |                   | 0.0049          |      |
| 5 <sup>c</sup>  | 1 + 1         | <sup>-</sup> CH <sub>2</sub> COOCH <sub>3</sub>               | CH <sub>3</sub> OH               |            | 1.0               | 178               |                   | 0.0056          |      |
| 6               | 2 + 2         | <sup>-</sup> CH <sub>2</sub> COOC <sub>2</sub> H <sub>5</sub> | C <sub>2</sub> D <sub>5</sub> OD | 15         | 4.2               | 163               | 0.092             | 0.026           | 3.49 |
| 7               | 2 + 2         | <sup>-</sup> CD <sub>2</sub> COOC <sub>2</sub> D <sub>5</sub> | C <sub>2</sub> H <sub>5</sub> OH | 32         | 4.5               | 167               | 0.19              | 0.027           | 7.18 |
| 8 <sup>c</sup>  | 2 + 2         | <sup>-</sup> CH <sub>2</sub> COOC <sub>2</sub> H <sub>5</sub> | C <sub>2</sub> H <sub>5</sub> OH |            | 3.8               | 169               |                   | 0.022           |      |
| 9               | 4 + 4         | <sup>-</sup> CH <sub>2</sub> COOC <sub>4</sub> H <sub>9</sub> | C <sub>4</sub> D <sub>9</sub> OD | 26         | 13                | 147               | 0.18              | 0.089           | 2.03 |
| 10              | 4 + 4         | <sup>-</sup> CD <sub>2</sub> COOC <sub>4</sub> H <sub>9</sub> | C <sub>4</sub> H <sub>9</sub> OH | 30         |                   | 152               | 0.20              |                 |      |
| 11 <sup>c</sup> | 4 + 4         | CH <sub>2</sub> COOC <sub>4</sub> H <sub>9</sub>              | C <sub>4</sub> H <sub>9</sub> OH |            | 8.8               | 152               |                   | 0.058           |      |

<sup>a</sup> Blank cells indicate no data available. <sup>b</sup> 10<sup>-11</sup> cm<sup>3</sup> molecule<sup>-1</sup> s<sup>-1</sup>. <sup>c</sup> Measured by Gross by monitoring the mono <sup>13</sup>C enolates reacting with counterpart alkyl alcohols.

observable reaction was proton transfer. TE reactions between isobutoxide and methyl acetate or ethyl acetate are exothermic. TE between isobutoxide and butyl acetate are very close to thermoneutral but cannot be detected under ICR because isobutoxide and *n*-butoxide have the same masses. TE reactions between methoxide and acetates are thermodynamically feasible, but no transesterified enolate ions were detected either. We confirmed the results reported earlier<sup>7,9</sup> that reactions between alkoxides and acetate esters undergo only proton transfer but not transesterification under typical ICR conditions.

**Theoretical Calculations.** Optimized geometries and energies of all species were obtained from density functional theory calculations with the Gaussian 98 program suite (Version 5.4) at the B3LYP/6-31++G\*\* level of theory. Vibrational frequency calculations were performed on the all optimized geometries. Energy minima and saddle points were confirmed by frequency analysis and by viewing the motion of the imaginary vibrational mode for transition states. The two critical transition states of TS and PE were further confirmed by the intrinsic reaction coordinate (IRC) procedures. For comparison, MP2 and CBS-QB3 calculations were also performed on these two species. When the reaction kinetics are modeled with RRKM theory, the B3LYP/6-31++G\*\* frequencies were used without scaling. The computer program HYDRA has been described elsewhere.<sup>23</sup> Important computational details can be found in the Discussion.

## Results

**Reaction Efficiencies and Rates.** Table 1 lists all rate constants and efficiencies. Although the reactions are thermoneutral, efficiencies are relatively high and easy to measure. Selected results of Gross<sup>9</sup> are also listed in Table 1 for direct comparison. Collision frequencies were calculated by the model of Su and Bowers.<sup>24</sup> TE rates ( $k_{TE}$ ) were measured by monitoring the disappearance of C1 + C2 + C3 and sums of two rates ( $k_{TE} + k_{PE}$ ) were measured by monitoring the disappearance of C1. This treatment implicitly neglects several secondary kinetic isotope effects. The correctness of the approximations and other important details of kinetic analysis are discussed in Supporting Information.

Gross first showed that rates of self-exchange TE reactions increase with the size of the alkyl group. It can be seen from our data that this is true not only for TE but also for PE. In addition, TE seems to increase faster, which causes  $k_{PE}/k_{TE}$  to decrease with the size of the alkyl group. Possible reasons will be discussed later. The rates from the two studies agree well, except for the TE rate between butyl enolate and butanol, in which a ~35% difference is observed. Both experiments suffer from the inaccuracy of absolute pressure measurements. The

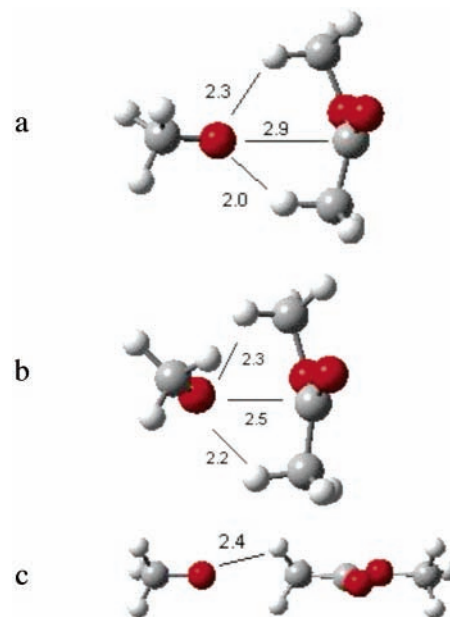


**Figure 1.** DFT structure of complex 6 (a), TSTE (b), and TSPE (c).

secondary isotope effects may also contribute to the disagreement (see Discussion and Supporting Information). Nevertheless, we believe that the  $k_{PE}/k_{TE}$  ratios reported here are more reliable because they are based on the exact same system. Most of the errors should cancel out including pressure measurements, which we consider to be the major error source.

**Potential Surface.** The potential surface of methyl acetate enolate anion and methanol was calculated with B3LYP/6-31++G\*\*. The critical structures of TSTE (transition state of TE), TSPE (transition state of PE), Complex 6 are shown in Figure 1. Energies of all important intermediates are shown in Figure 2. The only value that can be compared to experimental measurements is the difference in acidities of methyl acetate and methanol. Thermochemical data available from the NIST Webbook<sup>22</sup> yields a difference of 10.8 kcal/mol, which compares with the DFT predicted value of 8.3 kcal/mol (7.3 kcal/mol after ZPE correction). Complex 2 is a local minimum with all positive frequencies. But the TS3, which connects complex 2 and complex 1, is only 0.1 kcal/mol higher than complex 2. This is not uncommon in acid–base reactions.

## Discussion

Transesterification reactions are of fundamental importance in organic synthesis and in biology. They have been studied both in solution and in the gas phase. Most of gas phase experimental efforts have focused on esters without acidic

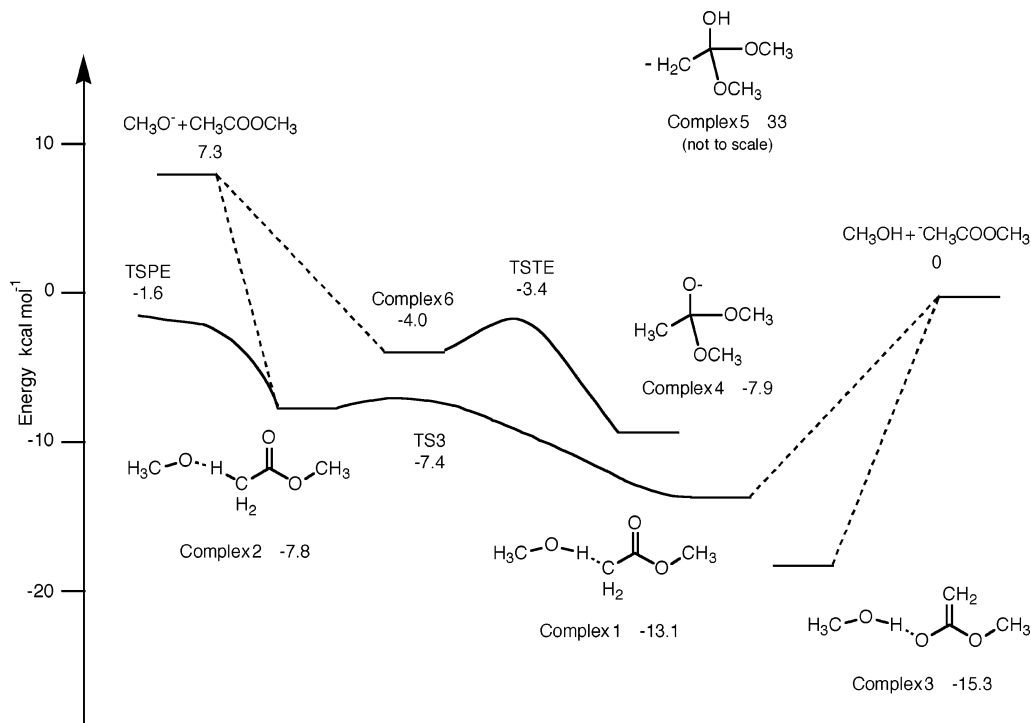
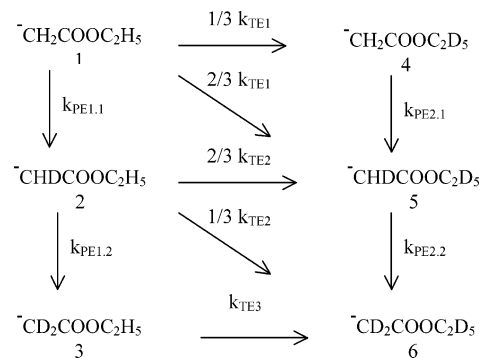


**Figure 2.** Potential surface of the reaction  $\text{CH}_3\text{O}^- + \text{CH}_3\text{COOCH}_3$ . The values below the species are ZPE corrected energies at B3LYP/6-31++G\*\* level.

$\alpha$ -hydrogens. The TE reactions are very fast and suggest that there is no significant barrier along the reaction coordinate. If there is an acidic  $\alpha$ -hydrogen, an even faster reaction, proton transfer, becomes dominant. Ion molecule reaction rates can yield useful information about the transition state energy only within a certain range (typically 0.1–20% efficiency). The lower end is usually limited by experimental inaccuracy. Volatile and highly reactive impurities are often the major source of error. The high end is often limited by dynamic problems and sensitivity of RRKM fitting. Sometimes efficiencies of highly reactive systems can be lowered to the informative range by taking advantage of one of the virtues of chemically activated systems: the same reactive system can be prepared with different energies or energy distributions by changing the reactants.<sup>25</sup> In our case, an endothermic proton transfer may serve as a useful method to cool the ion–molecule pair. Double hydrogen/deuterium exchange experiments, in which an endothermic proton transfer is followed by a hydrogen/deuterium exchange, has been shown to be informative compared with single hydrogen/deuterium exchange. For example, the *o*-difluorobenzene anion exchanges one hydrogen with  $\text{CH}_3\text{OD}$  but three hydrogens with  $\text{D}_2\text{O}$ , and the para isomer exchanges three hydrogens with  $\text{CH}_3\text{OD}$  but only one with  $\text{D}_2\text{O}$ .<sup>26</sup> In this case, the proton exchange with  $\text{CH}_3\text{OD}$  reveals the acidity only, whereas some dynamic information about the complexes can be found by the second proton exchange with  $\text{D}_2\text{O}$ . The same strategy can be adopted for transesterification reactions between enolates and alcohols. In both systems, the reaction procedure can be generalized as an endothermic proton transfer, followed by an exchange reaction, and an exothermic proton transfer. In enolate/alcohol reactions the second step is an alkoxide exchange, whereas in double hydrogen/deuterium exchange experiments, it is another proton exchange. The mechanism proposed by Gross and further supported by this study is shown below.

**Mechanisms and Kinetic Isotope Effects.** The physical mechanism is believed to be the one shown in Scheme 1 and

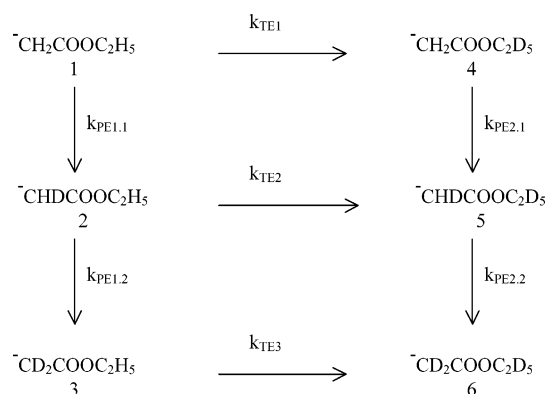
#### SCHEME 2: Mechanism I<sup>a</sup>



<sup>a</sup> System 3 is used as an example; the neutral alcohol is  $\text{DOC}_2\text{H}_5$  (not shown).

the corresponding phenomenological kinetic scheme is shown in Scheme 2. Here, hydrogen–deuterium exchange is assumed to be very fast, and thus statistical. The direct reaction paths from ion 1 to ion 5 (diagonal process in Scheme 2) and ion 2 to ion 6 clearly show that TE and PE happen in tandem. The three acidic hydrogens, one from the alcohol and two from the enolate, become indistinguishable. This strongly supports a relatively long-lived tetrahedral intermediate, and the reaction path includes both tetrahedral complex and hydrogen-bonded complex. In the other phenomenological kinetic scheme (Scheme 3), TE and PE are treated as independent processes. As a limiting case, this kinetic scheme is true only if TE can happen without PE (see later discussions). Our experiments achieve a satisfying fit only for Scheme 2 (see Supporting Information).

A tetrahedral intermediate has two identical (except isotope labeling) alkoxide groups and three  $\alpha$ -hydrogens. Transfer of one of the alkoxide groups gives transesterified products, and transfer of the other can give proton-exchanged products with 2/3 probabilities. Thus,  $k_{\text{PE,intrinsic}}$  is defined as  $k_{\text{PE}} - (2/3)k_{\text{TE}}$ . For all systems we studied,  $k_{\text{PE}}/k_{\text{TE}} > 2/3$ ,  $k_{\text{PE,intrinsic}} > 0$ . This requires another path to exchange the proton without trans-

SCHEME 3: Mechanism II<sup>a</sup>

<sup>a</sup> System 3 is used as an example; the neutral alcohol is  $\text{DOC}_2\text{H}_5$  (not shown).

esterification. The 2/3 correction factor comes from the number of exchangeable hydrogens/deuteriums. Strictly, this correction should be weighted by the selectivity of H and D, but we believe the selectivity is very close to unity (see Supporting Information for discussion).

Ideally, all rates listed in Scheme 2 can be fit from data, and most secondary kinetic isotope effects (KIE) can be calculated. However, the accuracy of the experimental data and fitting method prevent us from doing so. Another method to study some of KIE's is to compare mirror systems. For example, by comparing  $k_{\text{TE}}$  for systems 1 and 2 and for systems 3 and 4, secondary isotope effects for TE caused by isotopes on the alkyl group can be derived. Similarly, comparing  $k_{\text{PE}}$  for systems 1 and 2 and systems 3 and 4 will allow us to get the primary isotope effects for PE. This method, however, suffers from errors in absolute pressure measurements, obscuring relatively small KIEs. The ratios are also convoluted with secondary isotope ratios of alkyl groups from the alcohols. This makes interpretation even more difficult. All kinetic isotope effects mentioned above are nearly unity with one exception, the primary isotope ratio of PE for systems 3 and 4.<sup>21</sup> It appears that deuteriums on alkyl groups have little influence on TE rates, which agrees with our assumptions made in the kinetic analysis in the Supporting Information.

**Potential Surface.** Transesterification reactions have been studied less intensely than the comparable hydrolysis reactions. The first systematic quantum prediction was done by Ornstein and co-workers.<sup>10</sup> Potential surfaces of hydrolysis reactions of six representative esters were calculated. They focused on alkaline hydrolysis and did not calculate other reaction paths, for example, the Riveros reaction in case of methyl formate, and proton transfer reactions in case of acetate esters. These reactions dominate experimentally. The reaction between hydroxide and methyl formate was later studied in more detail by the Riveros group.<sup>11</sup> The loss of CO was included as well as hydrolysis of methyl formate. Authors of both papers later extended their systems to an even more challenging environment, the solution phase.<sup>27,28</sup>

In this work, we performed quantum calculations on gas phase reactions between methyl acetate and methoxide to obtain a more complete potential surface that is necessary for deeper understandings of the transesterification reactions of esters containing an acidic hydrogen. (Table 1, Figure 2). Ornstein's results first clearly show the most important feature of transesterification in the gas phase, an extremely shallow well along the reaction coordinate for hydroxide attacking acetyl carbon of acetate esters. We find a potential surface with a similar

feature in our system, where the attacking group is methoxide. The complex (noted as HBR1a in Figure 1 of ref 10, or complex 6 in this paper) at the bottom of the well is bound by ion-dipole interactions, stabilized by C-H-O interactions from both the acetyl and alkyl sides. Although Ornstein described the complex as hydrogen-bonded, these C-H-O interactions are probably not as strong as classical hydrogen bonds.<sup>10</sup> We prefer to designate this complex as an ion-dipole complex to avoid ambiguity with the more classical hydrogen-bonded complexes formed between methanol and acetate enolate (complex 1 and complex 3). Starting from the ion-dipole complex, the hydroxide or methoxide have to "push away" these alkyl groups to attack the carbonyl carbon. A barrier has to be overcome before the tetrahedral complex is formed. The same C-H-O interactions can be found at the top of the barrier, stabilizing the transition state (noted as TS1a in Figure 2 of ref 10 or TSTE in this paper). The barrier is very small, 1.1 and 0.4 kcal/mol for hydroxide and methoxide respectively, but it is crucial in determining reactivity of transesterification reaction, as shown later by RRKM calculations. Interestingly, a similar cage-like structure was found for methyl benzoate, which has a  $\beta$ -hydrogen, but not for methyl formate where a simple hydrogen-bonded complex is formed instead. The stability follows the trend: the hydrogen-bound complex (complexes 1 and 3) > the tetrahedral complex (complex 4) > the ion-dipole complex (complex 6). Complex 3 is overall the most stable species. Compared to complex 1, complex 3 is more stable because oxygen is more electron withdrawing than carbon. Ambident reactivity of enolate anions has been studied<sup>29-31</sup> by using special reagents to differentiate the products of carbon attack vs oxygen attack of enolate ions. In the transesterification reactions we examined here, oxygen attack followed by addition-elimination is very unlikely, because the corresponding tetrahedral complex (complex 5) is 33 kcal/mol higher in energy as predicted by DFT. More convincingly, if the reaction does go through this channel, mechanism II should be correct instead of mechanism I (Schemes 2 and 3). Thus, complex 3 is probably not on the reaction path for either PE or TE.

**TSTE (Transition State of Transesterification) and TSPE (Transition State of Proton Exchange).** The reaction paths for TE and PE are shown in Figures 2 and 3. TE is a symmetric triple well. Both the attacking group and the leaving group are methoxide. The potential surface will not be symmetric if there are different alkoxides or hydroxide, just as in the hydrolysis reactions calculated by Ornstein. The barrier of TSTE was fitted by RRKM theory to be -5.7 kcal/mol, about 2 kcal/mol lower than the DFT prediction. The surface for PE is a classical symmetric double well. The imaginary frequency of TSPE is like a wagging motion of methylene group, in which the attacking methoxide group sways from one  $\alpha$ -hydrogen to another, this ensures us that this is the saddle point for proton exchange. The experimental efficiency is about 3% ( $k_{\text{PE}} - (2/3)k_{\text{TE}}$ ). The barrier is fitted to be -3.4 kcal/mol. Again, this value is about 2 kcal/mol lower than that from the DFT calculation. This is unusual inasmuch as DFT appears to underestimate reaction barriers in most cases. Basis set tests were tried at B3LYP but no significant influence was found when basis set is larger than 6-31+\*. A few more resource-consuming quantum calculations were performed. MP2 gives nearly the same results as B3LYP, but CBS-QB3 predicts lower barriers and agrees better with RRKM. The results are listed in Table 2. Both transition states, especially TSPE, have a few very low frequencies.<sup>32</sup> They are more like internal rotations than harmonic oscillators, but it is not obvious what rotational

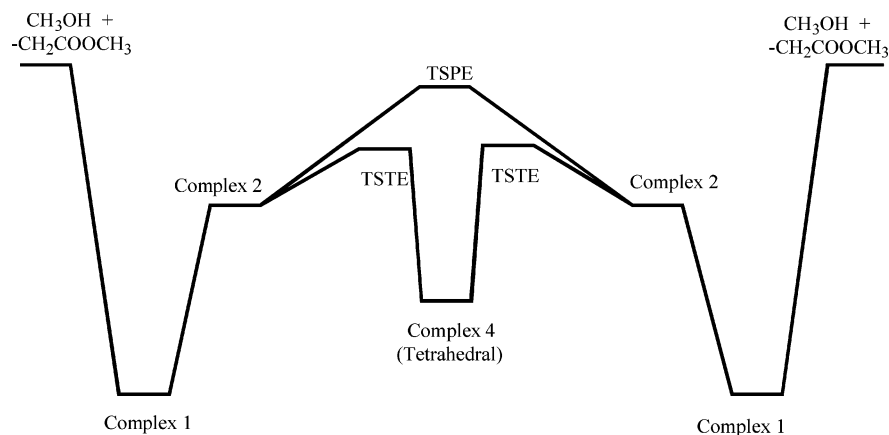


**Figure 3.** Reaction paths of TE and PE. (TS3, connecting complexes 1 and 2, is neglected).

**TABLE 2: Barrier Heights (kcal/mol) Relative to Methanol and Methyl Acetate Enolate**

|   | B3LYP/6-31++G** | MP2/6-311++G** | CBS-QB3 | ZPE  | RRKM |
|---|-----------------|----------------|---------|------|------|
| CH <sub>3</sub> O <sup>-</sup> + CH <sub>3</sub> COOCH <sub>3</sub> | 8.3             | 9.1            | 8.1     | -1.0 |      |
| TSST  | -3.6            | -4.7           | -6.3    | 0.2  | -5.7 |
| TSPE  | -0.9            | -0.4           | -1.3    | -0.7 | -3.4 |

constants should be used. The direct count method used in the RRKM program is expected to overestimate the efficiency. An anharmonic model should be more accurate but has not been used here. Tunneling has been neglected. Nevertheless, we believe that the reaction system can be understood within the framework of statistical theory and quantum calculations.

From Table 1 of ref 9, we see that when alcohols react with the same enolate, the TE rate has the order: *n*-BuOH > *n*-PrOH > *i*-PrOH ~ EtOH > MeOH. The reactivity correlates with acidities very well except for *i*-PrOH. This is actually an exothermicity-reactivity correlation, because alcohols have much different acidities than acetate esters with same alkyl groups. Steric effects may slow the rate of *i*-PrOH and explain the only exception. Rates of self-exchange reactions, which are thermo-neutral, follow the same trend: the bigger the alkyl group, the faster the reaction. The calculated geometry of TSST suggests that the C–H–O interactions exist between the oxygen atom on the attacking alkoxide and alkyl groups from both sides of the ester. These interactions are critical in stabilizing the TSST. It appears that the longer and more branched the alkyl group of the ester is, the stronger these C–H–O interactions are. Consequently, the TE reactions are favored kinetically, not thermodynamically, in these cases. We believe that it is the competition/combination of three factors (thermodynamic driving forces, steric effects, and stabilizing effects of alkyl groups, especially for branched ones) that determine the rate constants.

Both quantum calculations and RRKM theory predict that the TSPE is higher in energy than TSST, but the latter transition state is tighter. Overall, PE is faster than TE. We believe the major reason is that the TSST fixes both methyl rotations on the alkyl side and acetyl side, whereas TSPE leaves both of them free.

We also translationally accelerated the enolate anions.<sup>33</sup> However, because vibrational modes in enolate ions will also be activated in the low-energy collision processes, and energy transfer from translation to vibration is not quantitatively predictable, we cannot quantitatively analyze the dynamics. Nevertheless, the two channels can be directly compared because they must have the same extra energy. Both TE and PE rates decrease with increasing translational energy and TE slows down faster. The negative dependence with extra energy shows that both transition states are tight relative to the dissociation channel.

The faster slowing of TE suggests that TSST is tighter, just as predicted by theory.

In the reaction of methoxide and methyl acetate-*d*<sub>3</sub>, if any tetrahedral intermediate is formed in which undeuterated methoxide and deuterated methoxide are chemically equivalent, either methoxide should have a 50% chance to dissociate. If deuterated methoxide leaves, either deuterated methoxide or methyl acetate enolate (if a proton transfer follows the dissociation) should be detected. Because neither is observed in the experiment, we conclude that the reactants never enter this well. In systems 1 and 2, the efficiency of TSST is 0.0035, and the ratio *R* between the TE channel and the entrance or dissociation channel (methyl acetate enolate/methanol pair) can be derived from the reaction efficiency:  $\Phi = (k_{\text{diss}} + k_{\text{TE}}/k_{\text{diss}})$ ,  $R = k_{\text{TE}}/k_{\text{diss}} = \Phi/(1 - \Phi)$ . When the reaction is performed from the methoxide/methyl acetate pair, the methyl acetate enolate/methanol pair becomes another exit channel. The ratio *R* now determines the branching ratio between two exit channels: transesterification and proton transfer. TSST is a tight transition state, and the entrance channel (now the exit channel) is a loose one. It is expected that the higher the energy is, the lower the ratio is. Thus, no tetrahedral complex is formed when methyl acetate is attacked by methoxide. This suggests that even a very small barrier can prevent a reaction from happening when another channel is more facile. This phenomenon is not limited to this particular system. In the double hydrogen/deuterium exchange experiment, an anion can exchange two hydrogens with D<sub>2</sub>O. But if the reaction is performed using DO<sup>-</sup> with the corresponding neutral, simple proton transfer is the only observable product. This may also explain why transesterified products can be observed in a high-pressure CI source,<sup>9</sup> where the complexes may be collisionally stabilized.

## Conclusion

PE and TE are coupled in acetate enolates/alcohols reaction systems. The transesterification reaction is best viewed as an endothermic proton transfer, followed by an exchange of alkoxide and then an exothermic proton transfer. Quantum calculations were performed on methyl acetate and methoxide pair and only CBS-QB3 achieves satisfying agreement. Both RRKM and quantum calculations predict that the transition states

for transesterification reactions are the same for direct transesterification reactions between alkoxides and esters. A similar reaction scheme is suitable for double hydrogen/deuterium exchange experiments and may extend to other systems. An endothermic proton transfer, as an "ion cooling" method,<sup>34</sup> has a 2-fold advantage. It can adjust reaction efficiencies into an informative range, and slow, or even eliminate, otherwise accessible reaction channel(s).

**Acknowledgment.** We are grateful to the National Science Foundation for support of this work. X.C. is the recipient of a Stanford Graduate Fellowship.

**Supporting Information Available:** A more detailed analysis of the kinetics and the kinetic fit to the experimental data. This material is available free of charge via the Internet at <http://pubs.acs.org>.

## References and Notes

- (1) Page, M.; Williams, A. *Organic and Bio-organic Mechanisms*; Harlow: Longman, 1997.
- (2) McMurry, J. *Organic Chemistry*, 6th ed.; Thomson Brooks/Cole: Belmont, CA, 2004.
- (3) Bender, M. L. *Chem. Rev.* **1960**, *60*, 53.
- (4) Lee, K.; Sung, D. D. *Curr. Org. Chem.* **2004**, *8*, 557–567.
- (5) Asubiojo, O. I.; Brauman, J. I. *J. Am. Chem. Soc.* **1979**, *101*, 3715–3724.
- (6) Baer, S.; Stoutland, P. O.; Brauman, J. I. *J. Am. Chem. Soc.* **1989**, *111*, 4097–4098.
- (7) Vanderwel, H.; Nibbering, N. M. M. *Recl. Trav. Chim.* **1988**, *107*, 479–490.
- (8) Wilbur, J. L.; Brauman, J. I. *J. Am. Chem. Soc.* **1994**, *116*, 9216–9221.
- (9) Haas, G. W.; Giblin, D. E.; Gross, M. L. *Int. J. Mass Spectrom.* **1998**, *172*, 25–46.
- (10) Zhan, C. G.; Landry, D. W.; Ornstein, R. L. *J. Am. Chem. Soc.* **2000**, *122*, 1522–1530.
- (11) Pliego, J. R.; Riveros, J. M. *Chem.-Eur. J.* **2001**, *7*, 169–175.
- (12) Klass, G.; Underwood, D. J.; Bowie, J. H. *Aust. J. Chem.* **1981**, *34*, 507–517.
- (13) Frink, B. T.; Hadad, C. M. *J. Chem. Soc., Perkin Trans. 2* **1999**, 2397–2407.
- (14) Han, C. C.; Brauman, J. I. *J. Am. Chem. Soc.* **1989**, *111*, 6491–6496.
- (15) Riveros, J. M.; Ingemann, S.; Nibbering, N. M. M. *J. Chem. Soc., Perkin Trans. 2* **1991**, 1985–1989.
- (16) Riveros, J. M. *J. Chem. Soc., Chem. Commun.* **1990**, 773–774.
- (17) Jose, S. M.; Riveros, J. M. *Nouv. J. Chim.* **1977**, *1*, 113–119.
- (18) Ren, J. H.; Brauman, J. I. *J. Am. Chem. Soc.* **2004**, *3*, 2640–2646.
- (19) Walthall, D. A.; Chen, X.; Marcus, P.; Brauman, J. I. Manuscript in preparation.
- (20) Farneth, W. E.; Brauman, J. I. *J. Am. Chem. Soc.* **1976**, *98*, 7891–7898.
- (21) Ion balance is defined as the percentage of total ion intensity remaining at time  $t$  and is used to correct the unbiased ion loss process mass spectrometers.
- (22) <http://webbook.nist.gov/chemistry/>.
- (23) Wladkowski, B. D.; Lim, K. F.; Allen, W. D.; Brauman, J. I. HYDRA: Calculation of ion-molecular reaction rate coefficients using variational transition state theory. Details available from the authors.
- (24) Su, T.; Chesnavich, W. J. *J. Chem. Phys.* **1982**, *76*, 5183–5185.
- (25) Ferguson, E. E.; Smith, D.; Adams, N. G. *J. Chem. Phys.* **1984**, *81*, 742–747.
- (26) Kato, S.; DePuy, C. H.; Gronert, S.; Bierbaum, V. M. *J. Am. Soc. Mass Spectrom.* **1999**, *10*, 840–847.
- (27) Zhan, C. G.; Landry, D. W.; Ornstein, R. L. *J. Am. Chem. Soc.* **2000**, *122*, 2621–2627.
- (28) Pliego, J. R.; Riveros, J. M. *Chem.-Eur. J.* **2002**, *8*, 1945–1953.
- (29) Zhong, M. L.; Brauman, J. I. *J. Am. Chem. Soc.* **1996**, *118*, 636–641.
- (30) Brickhouse, M. D.; Squires, R. R. *J. Phys. Org. Chem.* **1989**, *2*, 389–409.
- (31) Freriks, I. L.; Dekoning, L. J.; Nibbering, N. M. M. *J. Am. Chem. Soc.* **1991**, *113*, 9119–9124.
- (32) The RRKM rate is very sensitive to low frequencies ( $<300\text{ cm}^{-1}$ ). For the PE channel, decreasing the frequencies by 10% can increase the RRKM reaction rate up to 25% without adjusting the reaction barrier. To fit the experimental rates, the corresponding barrier should be raised by up to 0.3 kcal/mol. This provides an estimation of the accuracy of RRKM fitting. Similar results also apply to TE channel but in a weaker way, because the low frequencies of the TSTE are fewer and relatively higher. Some of the frequencies can be replaced with methyl rotations, which usually change the rate by less than 20%.
- (33) Boering, K. A.; Rolfe, J.; Brauman, J. I. *Int. J. Mass. Spectrom. Ion Processes* **1992**, *117*, 357–386.
- (34) DePuy, C. H. *J. Org. Chem.* **2002**, *67*, 2393–2401.